

Pressure-induced phase transition in a molecule-based magnet with interpenetrating sublattices

Randy S. Fishman,¹ William W. Shum,^{2,3} and Joel S. Miller²

¹Materials Science and Technology Division, Oak Ridge National Laboratory, Oak Ridge, Tennessee 37831-6071, USA

²Department of Chemistry, University of Utah, Salt Lake City, Utah 84112-0850, USA

³Department of Chemistry, Cornell University, Ithaca, New York 14853, USA

(Received 8 March 2010; revised manuscript received 16 April 2010; published 21 May 2010)

The molecule-based magnet $[\text{Ru}_2(\text{O}_2\text{CMe})_4]_3[\text{Cr}(\text{CN})_6]$ contains two interpenetrating sublattices with sublattice moments confined to the cubic diagonals. At ambient pressure, a field of about 850 Oe rotates the antiferromagnetically coupled sublattice moments toward the field direction, producing a wasp-waisted magnetization curve. Up to 7 kbar, the sublattice moments increase with pressure due to the enhanced exchange coupling between the Cr(III) and Ru(II/III)₂ spins on each sublattice. Above 7 kbar, the sublattice moment drops by about half and the parallel linear susceptibility of each sublattice rises dramatically. The phase transition at 7 kbar is most likely caused by a high-to-low-spin transition on each Ru₂ complex.

DOI: 10.1103/PhysRevB.81.172407

PACS number(s): 75.50.Xx, 75.10.Dg, 75.30.Gw

Molecule-based materials provide the unprecedented opportunity to tune magnetic properties with choice of cation, guest molecules, or topology and by applying strain or pressure.¹ The molecule-based magnet $[\text{Ru}_2(\text{O}_2\text{CMe})_4]_3[\text{Cr}(\text{CN})_6]$ ($\text{Cr}(\text{Ru}_2)_3$) forms a body-centered-cubic structure with two interpenetrating cubic sublattices composed of alternating $S=3/2$ $[\text{Ru}_2(\text{O}_2\text{CMe})_4]^+$ (Ru_2) and $S=3/2$ $[\text{Cr}(\text{CN})_6]^{3-}$ (Cr) ions.² Due to the crystal field of the paddle-wheel complex sketched in the lower right of Fig. 1, the spin \mathbf{S} of each mixed-valent Ru(II/III)₂ ion³ experiences an easy-plane anisotropy $D(\mathbf{S}\cdot\mathbf{u})^2$, where $D \approx 8.6$ meV (Ref. 4) and \mathbf{u} bisects the paddle wheel along the Ru-Ru axis. The antiferromagnetic (AF) coupling J between the Cr(III) and Ru(II/III)₂ ions within each sublattice is much stronger than the AF coupling K between sublattices.

To our knowledge, $\text{Cr}(\text{Ru}_2)_3$ is the only material where two three-dimensionally ordered and weakly coupled magnetic sublattices occupy the same volume.

Because of the weak AF coupling K between sublattices, $\text{Cr}(\text{Ru}_2)_3$ undergoes a metamagnetic transition between AF and paramagnetic (PM) states at a critical field $H_c \sim K/\mu_B$. In ambient pressure, the metamagnetic transition is plotted in Fig. 1 for $T=8$ K. Shum *et al.*⁶ observed that the wasp-waisted magnetization curve of $\text{Cr}(\text{Ru}_2)_3$ sensitively depends on pressure. By 12.8 kbar, the constriction in the virgin curve has disappeared and any signature of the metamagnetic transition has vanished.

This Brief Report demonstrates that a phase transition separates a low-pressure (LP) phase below 7 kbar and a high-pressure (HP) phase above 7 kbar. In the LP phase, pressure enhances the coupling between sublattices and the sublattice moment grows. But in the HP phase, the sublattice moment falls dramatically and the susceptibility of each sublattice changes form.

Because of the easy-plane anisotropy on the Ru₂ complexes, each $\text{Cr}(\text{Ru}_2)_3$ sublattice is magnetically frustrated and a collinear magnetic ground state is not possible. In earlier work,⁵ we constructed the noncollinear magnetic ground state of each sublattice at ambient pressure. For the a , b , and c Ru₂ spins along the x , y , or z axes, the paddle wheels are perpendicular to the vectors $\mathbf{u}=\mathbf{x}$, \mathbf{y} , or \mathbf{z} . The proposed ground state is sketched in the upper left of Fig. 1: every Cr spin points along one of the eight cubic diagonals (accounting for orientation) and the sum of the Ru₂ a , b , and c spins points opposite the Cr spin. For infinite anisotropy and classical spins, the Ru₂ spins are confined to the easy plane of each paddle wheel; for finite anisotropy and quantum spins, the Ru₂ spins are canted toward the cubic diagonal but their expectation values are reduced in amplitude. For quantum spins with exchange coupling $J=D/5 \approx 1.7$ meV, the net sublattice spin is $M_{sl}=1.81$ per $\text{Cr}(\text{Ru}_2)_3$ unit cell at zero temperature (the net sublattice moment is $2\mu_B M_{sl}=3.62\mu_B$).

A model for the field and pressure dependence of the magnetization can be constructed based on the observation that the intersublattice coupling $K \sim 10^{-3}$ meV is much smaller than the intrasublattice coupling $J \sim 1$ meV (positive exchange is defined to be AF).⁵ At zero temperature, a net

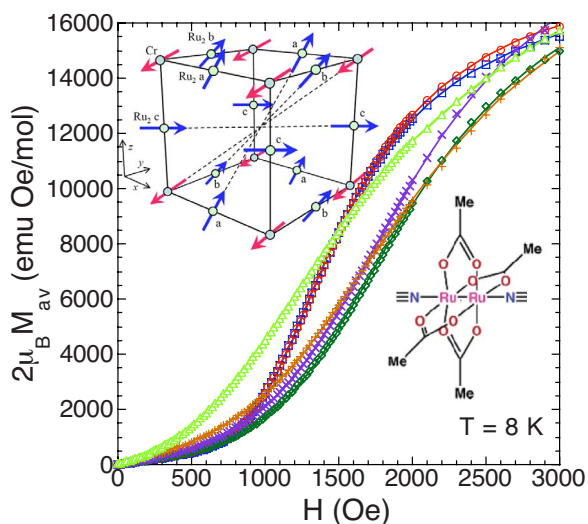


FIG. 1. (Color online) The initial magnetization (virgin curve) of polycrystalline $\text{Cr}(\text{Ru}_2)_3$ for $T=8$ K (Ref. 6) along with the predicted field dependence (solid curves) for several pressures: 1 bar (squares), 1.84 kbar (circles), 3.46 kbar (diamonds), 5.46 kbar (\times 's), 8.05 kbar ($+$'s), and 10.22 kbar (triangles). The proposed ground state (Ref. 5) of a single sublattice with classical spins and infinite anisotropy is sketched in the upper left; the Ru₂ paddle wheel is sketched in the lower right.

moment appears above the critical field $H_c \sim K/\mu_B \sim 1000$ Oe. Because $H_c \ll J/\mu_B \sim 10$ T, the magnetic ground state of each sublattice is only weakly perturbed by an external field up to several thousand Oersted. To a first approximation, the magnetic configuration of each sublattice can be considered to be rigid and the sublattice moment $j = 1$ or 2 can be written as $2\mu_B M_{sl}(T)\mathbf{n}_j$, where \mathbf{n}_j lies along one of the eight cubic diagonals.

Thermal equilibrium between the 64 possible configurations $\{\mathbf{n}_1, \mathbf{n}_2\}$ is achieved by fluctuations of the sublattice moments out of the completely ordered ground state. Below H_c , the ground state is AF with sublattice orientations $\mathbf{n}_1 = -\mathbf{n}_2$. Above H_c , the sublattice orientations \mathbf{n}_1 and \mathbf{n}_2 in the PM state lie along the cubic diagonals that are closest to the field direction \mathbf{m} .

The energy of a magnetic configuration with sublattice orientations $\{\mathbf{n}_{1i}, \mathbf{n}_{2i}\}$ on cluster i is given by

$$E = N_{Cr} \sum_i \{-\mu_B M_{sl}(\mathbf{n}_{1i} + \mathbf{n}_{2i}) \cdot \mathbf{H} + K M_{sl}^2 \mathbf{n}_{1i} \cdot \mathbf{n}_{2i}\}, \quad (1)$$

where $\mathbf{H} = H\mathbf{m}$ is the magnetic field and each cluster contains $N_{Cr} \propto \xi^3$ unit cells. The size ξ of a correlated magnetic cluster decreases as magnetic fluctuations are suppressed. Notice that the intrasublattice exchange J only enters this model implicitly through the sublattice spin $M_{sl}(T)$, which vanishes above $T_c \propto JS^2$. Compared to the model introduced in Ref. 5 with coupling energy $3S^2 K_c \mathbf{n}_{1i} \cdot \mathbf{n}_{2i}$, we now take $K \equiv 3S^2 K_c / M_{sl}^2$. This scaling removes the dominant temperature dependence from K_c .

While this model qualitatively describes $\text{Cr}(\text{Ru}_2)_3$, a quantitative description must also account for the small distortion of the sublattice ground state produced by the magnetic field. That distortion is responsible for two effects: the weak linear susceptibility $2\mu_B M/H$ observed within the AF state at low fields and the even weaker differential susceptibility $2\mu_B dM/dH$ observed within the PM state at high fields.

In a magnetic field \mathbf{H} , we assume that the susceptibility χ_{sl} of each sublattice moment $2\mu_B M_{sl}(\mathbf{H}, T)$ depends only on the angle $\theta = \arccos(\mathbf{n} \cdot \mathbf{m})$ between the cubic diagonal \mathbf{n} and the field direction \mathbf{m} ,

$$2\mu_B \mathbf{M}_{sl}(\mathbf{H}, T) = 2\mu_B M_{sl}(0, T)\mathbf{n} + \chi_{sl}(\theta)\mathbf{H}. \quad (2)$$

Expanding χ_{sl} in Legendre polynomials $P_l(\cos \theta)$ up to $l = 2$ produces the expression

$$\chi_{sl}(\theta) = \chi_0 + \chi_1 \sin^2(\theta/2) + \chi_2 \sin^4(\theta/2), \quad (3)$$

which ignores the weak dependence of χ_{sl} on the azimuthal angle ϕ about the cubic diagonal.

The first term χ_0 in Eq. (3) is the parallel susceptibility reflecting the induced magnetization along the direction of the sublattice moment \mathbf{n} with $\theta = 0$. In our earlier fits at ambient pressure,⁵ we took $\chi_0 = \chi_2 = 0$ and only retained χ_1 . We now keep all three terms subject to the constraint that $\chi_{sl}(\theta) \geq 0$ for any θ . As shown below, the experimental data is sufficiently discriminating to justify this more refined model and the pressure dependence of the parameters χ_n provides compelling evidence for a phase transition at 7 kbar.

With $\theta_j = \arccos(\mathbf{n}_j \cdot \mathbf{m})$, the noninteracting susceptibility

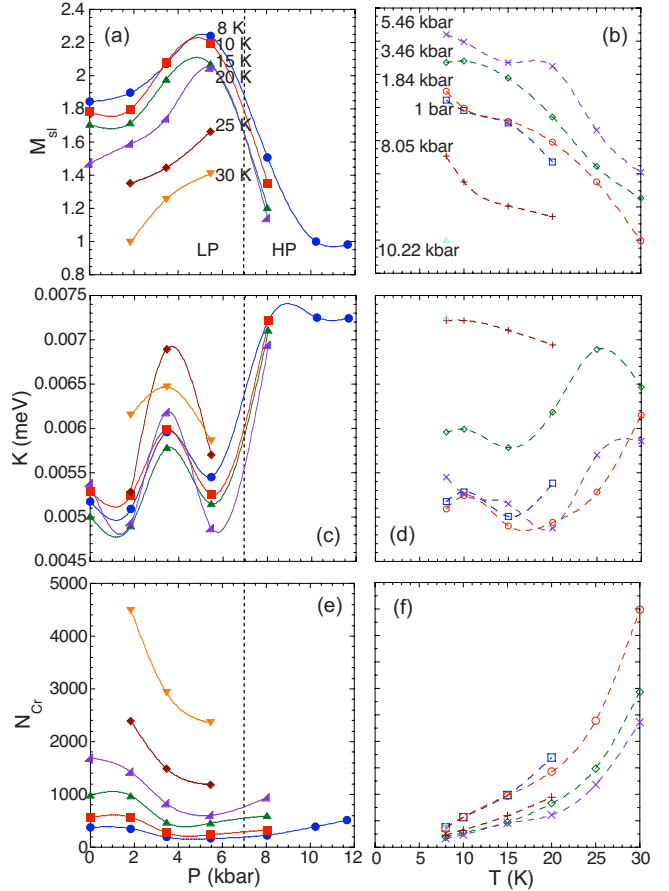


FIG. 2. (Color online) Fitting results as a function of pressure or temperature for (a) and (b) the sublattice spin M_{sl} , (c) and (d) the intersublattice exchange K (millielectron volt), and (e) and (f) the number N_{Cr} or Cr ions within a fluctuating magnetic cluster. Dashed vertical lines separate the LP and HP regions.

of the magnetic configuration $\{\mathbf{n}_1, \mathbf{n}_2\}$ is given by $\chi_{nint} = \chi_{sl}(\theta_1) + \chi_{sl}(\theta_2)$ per pair of Cr atoms. The additional linear term $N_{Cr} \chi_{nint} H/2$ is added to the magnetization and the extra term $-N_{Cr} \chi_{nint} H^2/4$ is added to the energy E of Eq. (1) for each cluster.

This model was used to evaluate the magnetization $2\mu_B M_{av}$ of a polycrystalline sample by averaging over field directions \mathbf{m} . For every temperature T , M_{av} depends on six parameters: the three components of the sublattice susceptibility χ_n , the sublattice spin M_{sl} , the weak AF interaction K between sublattices, and the number N_{Cr} of $\text{Cr}(\text{Ru}_2)_3$ unit cells within each cluster (half belonging to each sublattice). For $T = 8$ K, the resulting fits are plotted in Fig. 1.⁷ For temperatures up to 30 K and pressures up to 11.7 kbar, M_{sl} , K , and N_{Cr} are plotted in Fig. 2.

Generally, these fits break down close to T_c and at high fields because the field-induced change $\chi_{sl}(\theta)H$ in each sublattice moment becomes a substantial fraction of the zero-field moment $2\mu_B M_{sl}(0, T)$.⁷ In other words, the sublattice ground state can no longer be considered to be rigid near T_c or for high fields.

The fitting parameters show a marked change at 7 kbar. In the LP phase below 7 kbar, applied pressure has the expected effect of enhancing the intrasublattice exchange J compared

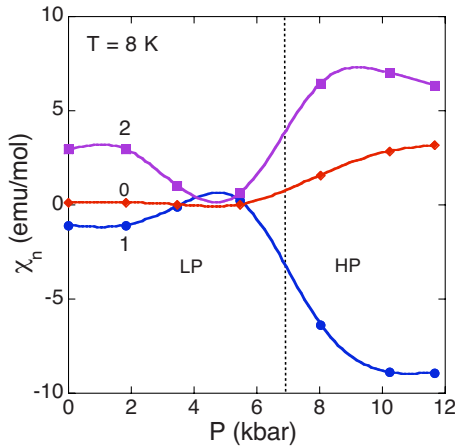


FIG. 3. (Color online) The three components χ_n ($n=0, 1$, and 2) of the sublattice susceptibility $\chi_{sl}(\theta)$ versus pressure at 8 K.

to the anisotropy D of the Ru_2 paddle-wheel complex. Consequently, the sublattice spin M_{sl} plotted in Fig. 2(a) increases with pressure in the LP phase. At 8 K, M_{sl} increases from 1.8 to 2.2 between ambient pressure and 5.46 kbar. To explain this enhancement, J must be increased by about 60% and D/J lowered from 5 to 3. The increase in J is also reflected in the growth of T_c from 33 to 42 K.⁶ Notice that $M_{sl}(T)$ shows the expected reduction with temperature in Fig. 2(b). By contrast, K is relatively insensitive to temperature for each pressure below about 25 K, as expected for the rescaled intersublattice exchange introduced in Eq. (1).

As shown by the reduction in $N_{\text{Cr}} \sim \xi^3$ with increasing pressure below 7 kbar in Fig. 2(e), pressure initially suppresses the size ξ of the fluctuating magnetic clusters. With increasing temperature, critical fluctuations produce the exponential dependence $N_{\text{Cr}}(T) \propto (1 - T/T_c)^{-3\nu}$ seen in Fig. 2(f). Our results remain consistent with a mean-field-like critical exponent $\nu=1/2$ for all pressures. In $\text{Cr}(\text{Ru}_2)_3$, the magnetic correlation length ξ can be estimated directly from the magnetization rather than from elastic neutron-scattering measurements.

In the HP phase above 7 kbar, the sublattice spin M_{sl} drops dramatically. At low temperatures, M_{sl} in Fig. 2(a) drops from about 2.2 at 5.46 kbar to 1 at 10.22 kbar. The intersublattice exchange K plotted in Fig. 2(c) peaks at about 4 kbar but then rises by roughly 20% above 7 kbar. Somewhat less dramatically, Fig. 2(e) indicates that N_{Cr} also grows above 7 kbar, suggesting that thermal fluctuations are enhanced in the HP phase.

The linear susceptibility of each sublattice plotted in Fig. 3 also shows a dramatic change at 7 kbar. In the LP phase, the parallel susceptibility χ_0 is rather small and can be taken to be zero. Notice that the sublattice ground state becomes *more* rigid with increasing pressure below 7 kbar as the susceptibilities χ_n decrease in amplitude. Above 7 kbar, χ_0 becomes non-negligible and the magnitudes of χ_1 and χ_2 are significantly enhanced. For all pressures, $\chi_1 < 0$ and $\chi_2 > 0$.

We conclude that the atomic spins are more easily rotated by a magnetic field along the sublattice moment direction ($\theta=0$) in the HP phase above 7 kbar than in the LP phase below 7 kbar. Since the LP-HP transition is first order, it is

very likely that the material exhibits phase separation at 8.05 kbar with both LP and HP regions. Hence, the apparent reduction in M_{sl} at 8 K between 8.05 and 10.22 kbar probably reflects the disappearance of the LP phase rather than a change in the net sublattice spin within the HP phase. So the sublattice spin of the HP phase at low temperatures lies between about 0.9 and 1.1. Despite the very small 0.45% tetragonal expansion of the lattice observed at 12.2 kbar,⁶ any canting of the sublattice moments away from the cubic diagonals in the HP phase is negligible: when the canting angle is allowed to be a variable in the fits to the magnetization, the net moment is always found along one of the cubic diagonals.

Based on these considerations, there are two possible explanations for the LP-HP phase transition. Pressure-induced valence changes have been previously observed among mixed-valent rare-earth compounds⁸ and intermetallic oxides.⁹ Applied pressure may also induce a valence change on one of the three inequivalent Ru_2 complexes, reducing its spin from $3/2$ to 1. The Cr ion would gain the electron removed from this Ru_2 complex. Due to the surrounding six cyanide groups, the Cr(II) ion would likely support a low-spin state with $S=1$. But the sublattice moment would then still be too large compared to the result $M_{sl} \approx 1$ expected for the HP phase.

Many compounds, including those containing Fe, Co, or Mn ions, exhibit a high-to-low-spin transition with increasing pressure.¹⁰ If the Ru_2 complex undergoes a high-to-low-spin transition, then the Ru_2 spin would change from $3/2$ to $1/2$. In the absence of spin-orbit coupling, the spin- $1/2$ Ru_2 ion would be decoupled from the crystal-field environment and the net sublattice moment would vanish. But due to the spin-orbit coupling $\lambda < 0$, the Ru_2 moment would couple to the crystal field of the paddle wheel. The net sublattice moment would then be substantially reduced from its value in the LP phase and, depending on the magnitude of the Ru_2 moment, may lie either parallel or antiparallel to the Cr moments. Considering that the different orbital configurations of the Ru_2 core have nearly the same energy,¹¹ it is not surprising that both low-spin¹² and spin-admixed¹³ diruthenium compounds are fairly common. Thus, $\text{Cr}(\text{Ru}_2)_3$ would provide an example of a pressure-induced high-to-low-spin transition for a diruthenium compound.

To summarize, we have modeled the magnetization of $\text{Cr}(\text{Ru}_2)_3$ as a function of field and pressure. Up to 7 kbar, the magnetization grows with increasing pressure due to the enhanced coupling between spins. Above 7 kbar, the sublattice moment drops by a factor of 2 and the linear susceptibility of each sublattice along the cubic diagonal rises dramatically. Of the two scenarios described above, it is most likely that the Ru_2 ion undergoes a high-to-low-spin transition at 7 kbar. Further measurements are needed to verify this prediction. It would also be interesting to study the pressure dependence of the two-dimensional analog of $\text{Cr}(\text{Ru}_2)_3$.¹⁴

We would like to acknowledge helpful discussions with Satoshi Okamoto. This research was sponsored by the Division of Materials Sciences and Engineering of the U.S. Department of Energy (R.S.F.) and by the U.S. National Science Foundation (Grant No. 0553573) (W.W.S. and J.S.M.).

- ¹J. S. Miller and A. J. Epstein, *Angew. Chem., Int. Ed. Engl.* **33**, 385 (1994); J. S. Miller and A. J. Epstein, *MRS Bull.* **25**, 21 (2000); J. S. Miller, *Adv. Mater.* **14**, 1105 (2002).
- ²Y. Liao, W. W. Shum, and J. S. Miller, *J. Am. Chem. Soc.* **124**, 9336 (2002).
- ³V. M. Miskowiski, M. D. Hopkins, J. R. Winkler, and H. B. Gray, in *Inorganic Electronic Structure and Spectroscopy*, edited by E. I. Solomon and A. B. P. Lever (Wiley, New York, 1999), Vol. 2, Chap. 6.
- ⁴W. W. Shum, Y. Liao, and J. S. Miller, *J. Phys. Chem. A* **108**, 7460 (2004).
- ⁵R. S. Fishman, S. Okamoto, W. W. Shum, and J. S. Miller, *Phys. Rev. B* **80**, 064401 (2009).
- ⁶W. W. Shum, J.-H. Her, P. W. Stephens, Y. Lee, and J. S. Miller, *Adv. Mater.* **19**, 2910 (2007).
- ⁷The virgin magnetization curves contain a constant magnetization at zero field. This constant is simply added to the theoretical result. Fits were performed using different cutoff fields. The resulting fitting parameters were averaged over all fits where the maximum increase $\chi_{sl}H$ in the sublattice moment with field was smaller than $1.2\mu_B M_{sl}(H=0, T)$.
- ⁸A. Jayaraman, W. Lowe, and L. D. Longinotti, *Phys. Rev. Lett.* **36**, 366 (1976); B. Perscheid, E. V. Sampathkumaran, and G. Kaindl, *J. Magn. Magn. Mater.* **47-48**, 410 (1985); A. T. Holmes, D. Jaccard, and K. Miyake, *Phys. Rev. B* **69**, 024508 (2004).
- ⁹B. J. Kennedy, L. Li, Y. Lee, and T. Vogt, *J. Phys.: Condens. Matter* **16**, 3295 (2004); M. Azuma, S. Carlsson, J. Rodgers, M. Tucker, M. Tsujimoto, S. Ishiwata, S. Isoda, Y. Shimakawa, M. Takano, and J. P. Attfield, *J. Am. Chem. Soc.* **129**, 14433 (2007).
- ¹⁰M. Takano, S. Nasu, T. Abe, K. Yamamoto, S. Endo, Y. Takeda, and J. B. Goodenough, *Phys. Rev. Lett.* **67**, 3267 (1991); J.-P. Rueff, C.-C. Kao, V. V. Struzhkin, J. Badro, J. Shu, R. J. Hemley, and H. K. Mao, *ibid.* **82**, 3284 (1999); F. Aguado, F. Rodriguez, and P. Núñez, *Phys. Rev. B* **76**, 094417 (2007); N. O. Golosova, D. P. Kozlenko, L. S. Dubrovinsky, O. A. Drozhzhin, S. Ya. Istomin, and B. N. Savenko, *ibid.* **79**, 104431 (2009).
- ¹¹P. Angaridis, F. A. Cotton, C. A. Murillo, D. Villagrán, and X. Wang, *J. Am. Chem. Soc.* **127**, 5008 (2005).
- ¹²J. L. Bear, B. Han, S. Huang, and K. M. Kadish, *Inorg. Chem.* **35**, 3012 (1996); W.-Z. Chen and T. Ren, *ibid.* **42**, 8847 (2003); M. C. Barral, R. González-Prieto, S. Herrero, R. Jiménez-Aparicio, J. L. Priego, E. C. Royer, M. R. Torres, and F. A. Urbanos, *Polyhedron* **23**, 2637 (2004).
- ¹³M. C. Barral, S. Herrero, R. Jiménez-Aparicio, M. R. Torres, and F. A. Urbanos, *Angew. Chem., Int. Ed.* **44**, 305 (2005); M. C. Barral, T. Gallo, S. Herrero, R. Jiménez-Aparicio, M. R. Torres, and F. A. Urbanos, *Chem.-Eur. J.* **13**, 10088 (2007).
- ¹⁴T. W. Vos and J. S. Miller, *Angew. Chem., Int. Ed.* **44**, 2416 (2005); R. S. Fishman, S. Okamoto, and J. S. Miller, *Phys. Rev. B* **80**, 140416(R) (2009).